Detailed luminescence spectra interpretation of selected oxides: spinel from Myanmar and chrysoberyl – var. alexandrite from Tanzania

Iveta Malíčková[1], Peter Bačík[1,2], Jana Fridrichová[1], Radek Hanus[3], Ján Štubňa[4], Stanislava Milovská[5], Radek Škoda[6]

[1] Comenius University, Faculty of Natural Sciences, Department of Mineralogy and Petrology, Ilkovičova 6, 842 15 Bratislava, Slovakia, malickova3@uniba.sk, peter.bacik@uniba.sk, jana.fridrichova@uniba.sk
[2] Earth Science Institute of the Slovak Academy of Science, Dúbravska cesta 9, 840 05, Bratislava, Slovakia
[3] Gemological Laboratory of e–gems.cz, 110 00 Prague, Czech Republic; kakt@centrum.cz
[4] Gemmological Institute, Faculty of Natural Sciences, Constantine the Philosopher University in Nitra, Nábrežie mládeže 91, 949 74 Nitra, Slovakia; jstubna@ukf.sk
[5] Earth Science Institute of the Slovak Academy of Sciences, Ďumbierska 1, 974 01 Banská Bystrica, Slovakia; milovska@savbb.sk
[6] Masaryk University, Faculty of Science, Department of Geological Sciences, Kotlářská 2, 611 37 Brno, Czech Republic; rskoda@sci.muni.cz

AGEOS

Abstract: Different structure and symmetry of spinel and chrysoberyl influence their luminescence spectra Observed with Raman spectroscopy. Luminescence bands of spinel at 677, 685, 697, 710 a 718 nm were assigned to Cr^{3+}. Luminescence duplet located at 685 and 687 nm belongs to R_1 and R_2–lines for the Cr^{3+} ion, the electron transition $^2Eg \rightarrow {}^4A_{2g}$, N_1 and N_4 at 687 and 700 nm; N_3 (689 nm) is weak. Luminescence centers of alexandrite located at 644, 650, 653, 667, 669, 678, 680, 690, 694, 702, 707, and 716 nm were assigned to Cr^{3+}. R–lines assigned to 679 with 677.3 nm, and 694.4 with 691.7 nm, accompanied by N–lines of Cr–Cr pairs. Luminescent duplet of alexandrite at 680 nm is associated with electron transition $^2Eg \rightarrow {}^4A_{2g}$. The R–lines in chrysoberyl are located at 678 nm (R_m–line) a 690 nm (R_i–line). Lower symmetry of the structure and Cr^{3+}–bearing octahedra results in splitting, widening and overlapping of the luminescence bands in spectrum. Spinel with higher symmetry than chrysoberyl has the luminescence spectrum with smaller number of better resolved bands.

Key words: luminescence, Raman Spectroscopy, spin–forbidden transition, spinel, alexandrite

1. INTRODUCTION

The spinel–supergroup minerals have the general formula AB_2X_4, where A represents divalent and B trivalent cations at the tetrahedrally and octahedrally coordinated sites of a structure with a cubic nearly close–packed arrangement (Bosi et al., 2019). In spinel, the A site is occupied by Mg, B site contains Al and the X site is occupied by O. Most natural and synthetic spinels are disordered, Al occupies tetrahedral site and both Al and Mg occupies octahedral sites (Fig. 1A). This disorder causes defects, electron traps and vacancies in the crystal structure that complicate the interpretation of the spectra (Cynn et al., 1992).

Chrysoberyl, $BeAl_2O_4$, is orthorhombic, space group *Pbmn* (Anthony et al., 2017). The chrysoberyl crystal structure is similar to that of spinel but has reduced symmetry. It results from the different cation sizes – Be^{2+} is significantly smaller cation than Al^{3+} (Shannon, 1976). Beryllium occupies tetrahedra and Al occupies two types of slightly distorted interstitial octahedral sites: B1 octahedra of C_i symmetry and B2 octahedra of C_s symmetry (Hawthorne & Huminicki, 2002). These octahedra have different volume, B2 is larger than B1 (Fig. 1B). Substitutions of Cr^{3+} and Fe^{3+} ions replace Al^{3+}. Numerous experiments indicate uneven distribution of cations between two non–equivalent octahedral sites in the chrysoberyl structure (Yeom et al., 1998; Yeom & Choh, 2001; Weber et al., 2007). The most intensive luminescence duplet at 680 nm is caused by high Cr^{3+} content at the B2 site with C_s symmetry , about 70 % of the chromium is the present there (Bordage et al., 2012). Ferric iron prefers the more symmetrical B1 site whereas trivalent chromium cations that cause the color of alexandrite (Cr-bearing variety of chrysoberyl) occupy the B2 site (Urusov et al., 2011).

The luminescence properties, radiation transition characteristics as well as emissions at selective site excitation depend on the symmetry of the luminescence center environment (Gaft et al., 2005). The goal of this study is to compare luminescence spectra of spinel and chrysoberyl – var. alexandrite, which both can accommodate Cr^{3+} as luminophore. They are structurally relatively similar but the slight structural differences allow to study the dependence of the luminescence spectra complexity on the mineral structure and symmetry.

2. MATERIALS AND METHODS

We studied two crystal fragments of natural samples of red Cr-bearing spinel from Mogok, Myanmar (SPM–1) and yellow-green Cr-bearing chrysoberyl, var. alexandrite, from Lake Manyara, Tanzania (ALM–1). The measured Raman spectra differ from the published data by absence of some vibrations, depending on the sample orientation relative to the laser beam. Spectra of studied samples were measured with the random orientation because it was not possible to determine orientation on the irregular crystal fragments.

Raman spectroscopy was performed by LabRAM–HR Evolution (Horiba Jobin–Yvon) spectrometer system with a Peltier cooled CCD detector and Olympus BX–41 microscope (Masaryk University, Department of Geological Sciences). Raman spectra were excited by 473 nm frequency–doubled diode laser
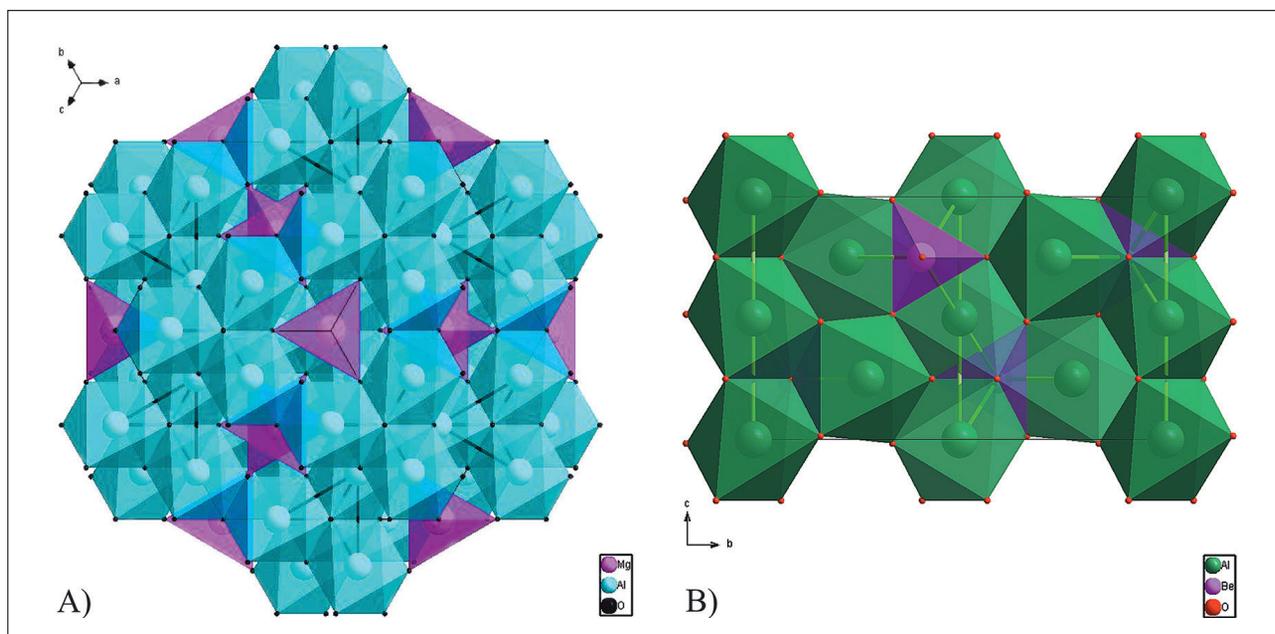
Fig. 1. Crystal structure of the spinel (SPM–1) (A) (Peterson et al., 1991), and the chrysoberyl – var. alexandrite (B) (Hazen, 1987).

and a 520.6 cm^{-1} silicon wafer was used for spectral calibration. Spectra ranged from 100 to 10,000 cm^{-1} with acquisition time of 15 s per frame, 2 accumulations and were dispersed by diffraction grating with 600 grooves per mm. Raman spectra were processed in Seasolve PeakFit 4.1.12 software. Raman bands were fitted by Lorentz function with automatic background correction and Savitzky–Golay smoothing.

Chemical composition (Tab. 1) was determined by energy-dispersive micro X–ray fluorescence spectroscopy (micro–XRF) using an instrument M4 TORNADO, Bruker (Earth Science Institute of the Slovak Academy of Science, Banská Bystrica). Incident X–ray beam (Rh anode) was focused by polycapillary optics to 25–micron spot, interaction depth was ca. 10–1000 μm, excitation current 600 μA at 50 kV. Analyses were acquired at 20 mbar vacuum. A silicon drift detector (SDD) collecting the fluorescence signal has an active area 30 mm^2 and spectral

resolution 145 e. Measuring time of point analyses was 70 s, live time 60 s, energy range of 0.25–20 keV. Element concentrations were computed by fundamental-parameters method.

3. RESULTS

3.1. Chemical composition

Results obtained from XRF analysis were not converted to crystal–chemical formula but are reported in wt. % because the measured data do not have sufficient precision for calculation of the stoichiometric formula.

The most abundant element in the spinel samples is Al_2O_3 (68.36 wt. %), MgO (24.23 wt. %), corresponding to the spinel formula. Spinel is enriched in Cr_2O_3 (3.96 wt. %), V_2O_3 (0.63 wt. %), FeO (0.15 wt. %), and TiO_2 (0.07 wt. %). Other elements such as SiO_2 (0.79 wt. %), CaO (0.50 wt. %) are probably bound in the form of microscopic impurities.

In the chrysoberyl sample, Al_2O_3 (90.28 wt. %) is the most abundant, Be was not analyzed. Chrysoberyl is also enriched in FeO (2.63 wt. %), TiO_2 (0.81 wt. %), Cr_2O_3 (0.72 wt. %), CaO (0.71 wt. %), MgO (0.31 wt. %), and SiO_2 (0.14 wt. %) occur in a smaller amount.

3.2. Raman spectra

Raman bands of spinel (Fig. 2A) were assigned according to Weigi et al. (1985) and Slotznick & Shim (2008): the 307 and 662 cm^{-1} bands are attributed to T_{2g} symmetry, 403 cm^{-1} band to E_g, and 763 cm^{-1} to A_{1g} symmetry (Tab. 2). The measured values deviate up to 5 cm^{-1} from the published data (citace).

The Raman bands of chrysoberyl (Fig. 2B) were assigned according to Weigi et al. (1985). The Raman 240, 369, 460, 522,

Tab. 1. Results of X–ray fluorescence analysis of the studied samples. S. D. – standard deviation on 1 sigma.

	SPM–1	ALM–1	S. D.
SiO_2	0.79	0.14	0.32
TiO_2	0.07	0.81	0.01
Al_2O_3	68.36	90.28	0.11
Cr_2O_3	3.96	0.72	0.13
V_2O_3	0.63	0.00	0.03
FeO	0.15	2.63	0.10
MnO	0.02	0.00	0.001
MgO	24.23	0.31	1.13
NiO	0.01	0.04	0.01
SrO	0.02	0.02	0.01
CaO	0.50	0.71	0.16
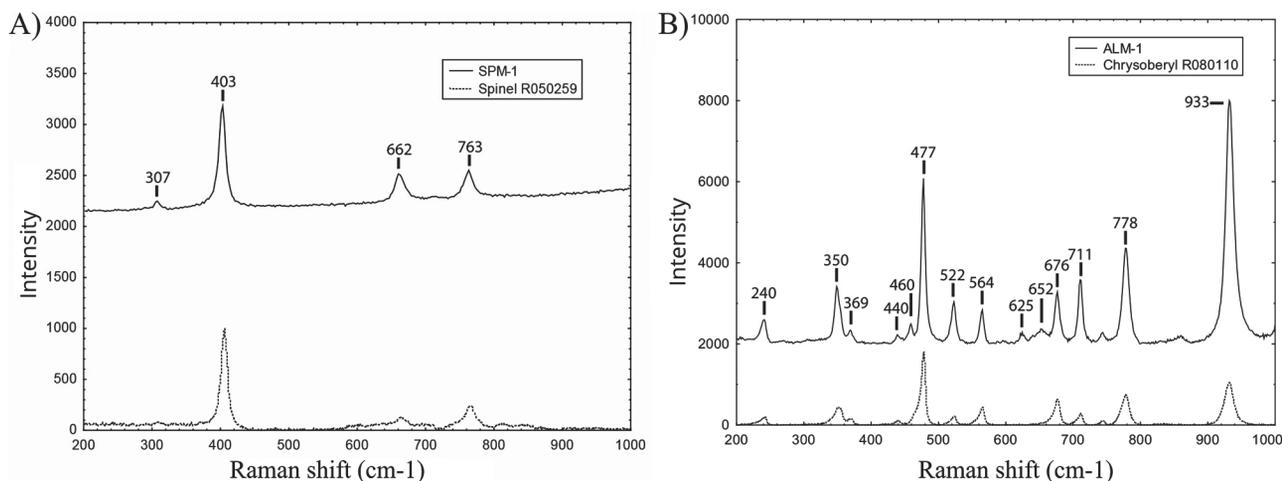
Fig. 2. Raman spectra of the spinel (SPM–1) (A), the chrysoberyl – var. alexandrite (ALM–1) (B).

625, 711, and 778 cm^{-1} bands belong to A$_g$, 350 and 933 cm^{-1} bands belong to B$_{2g}$, 440 and 652 cm^{-1} bands belong to B$_{1g}$, and 477, 564, and 676 cm^{-1} bands belong to B$_{3g}$ symmetry (Tab. 2). The measured values differ up to 3–8 cm^{-1} from the published data (Weigi et al., 1985; Burshtein et al., 1989).

3.3. Luminescence spectra

The most intensive region in the luminescence spectrum of spinel is from 673 to 725 nm, with the most intensive bands located at 671, 673, 677, 685, 687, 697, 699, 700, 705, 706, 710, 718, and 722 nm. The individual bands are well defined. The most intensive split band at the 685 nm belongs to the R–lines, whereas other luminescence bands are attributed to the N–lines. Luminescence bands at 677, 685, 697, 710, and 718 nm were assigned to Cr^{3+} according to Gaft et al. (2005).

Tab. 2. Raman shifts (cm^{-1}) of Raman–active bands in the studied sample. Assignment of the spinel band modes was made according to Slotznick & Shim (2008) and chrysoberyl – var. alexandritu (ALM–1) band modes was made according to Weigi etal. (1985).

Symmetry	SPM-1	Symmetry	Vibrations	ALM-1
T$_{2g}$	307	A$_g$	Lattice vibration	240
E$_g$	403	B$_{2g}$	Lattice vibration	350
T$_{2g}$	662	A$_g$	Lattice vibration	369
A$_{1g}$	763	B$_{1g}$	Lattice vibration	440
		A$_g$	Lattice vibration	460
		B$_{3g}$	Lattice vibration	477
		A$_g$	Bending vibration	522
		B$_{3g}$	Bending vibration	564
		A$_g$	Bending vibration	625
		B$_{1g}$	Bending vibration	652
		B$_{3g}$	Bending vibration	676
		A$_g$	Stretching vibration	711
		A$_g$	Stretching vibration	778
		B$_{2g}$	Stretching vibration	933

The luminescence spectrum of chrysoberyl comprises broad bands in the range from 640 to 780 nm. The best resolved luminescence bands at 644, 650, 653, 667, 669, 678, 680, 690, 694, 702, 707, and 716 nm were assigned to Cr^{3+}. However, the bands are overlapped mostly in regions of 650–680 nm and 690–720 nm (Gaft et al., 2005). The R–lines range from 644 to 694 nm and the N–lines are located between 702 and 716 nm.

4. DISCUSSION

4.1. Luminescence spectroscopy of spinel

Luminescence features were observed in the Raman spectrum of spinel. Luminescence centers (Fig. 3A) at 677, 685, 697, 710, and 718 nm were assigned to Cr^{3+} (Gaft et al., 2005).

The luminescence spectrum of spinel usually has three parts: (a) The purely electronic R–lines, assigned collectively to the most intense centers (Mohler & White, 1995); (b) a series of N–lines (Stokes or anti–Stokes line) associated with eight Cr^{3+}–Cr^{3+} pair interactions and with Cr^{3+} at sites differing from the primary site, the concentration–dependent N–lines are caused by chromium pairs, the structure–dependent N–lines arise from six coordinated Cr^{3+} ions whose short-range orders are distorted (Derkosch et al., 1977); (c) series of phonon side bands on the tow energy side of the R–lines that relate to the vibrational modes of the spinel crystal (Mohler & White, 1995). N–lines generally arise from different kinds of luminescence centers compared to R–lines. As there is no doubt that Cr^{3+} ions are the actual luminescent species in each case, the differences must result from the local environments of the Cr^{3+} ions. The spectra of chromium–bearing spinel are usually dominated by R–lines indicating the host lattice being entirely well ordered (Mikenda & Preisinger, 1981[a]; Mikenda & Preisinger, 1981[b]).

The most intensive luminescence duplet of the studied sample, which is located at 685 and 687 nm belong to R$_1$ and R$_2$–lines and arises from the states of the Cr^{3+} ion in an ideal short–range order due to the spin–forbidden transition $^2E_g \rightarrow {}^4A_{2g}$ (Mikenda & Preisinger, 1981[a]; Mikenda & Preisinger, 1981[b]). In addition to R–line, N$_1$ and N$_4$ lines at 687 and 700 nm were also detected;
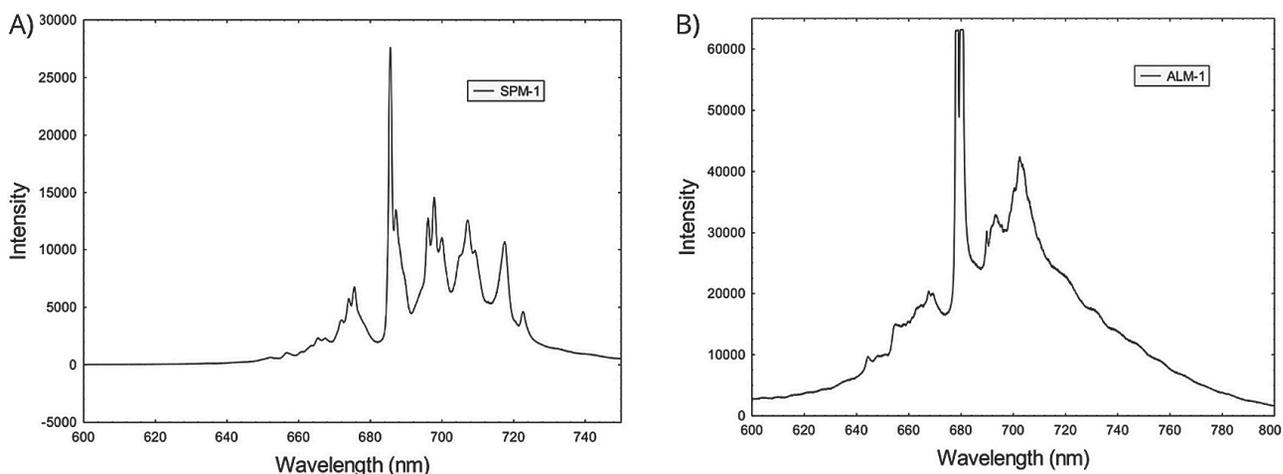
Fig. 3. Luminescence spectra of the spinel (SPM–1) (A), the chrysoberyl – var. alexandrite (ALM–1) (B).

N_3 (689 nm) is weak. The N_1 and N_3 lines are related to a coupling between the Cr^{3+} state and lattice defect, while N_4 pertains to interaction of the Cr^{3+}– Cr^{3+} pairs. The intensity of these lines increases with the Cr^{3+} concentration (Phan et al., 2004). The N_3–line is weak, it is probably due to a weak interaction of the pairs and the distribution of Cr^{3+} in the structure.

4.2. Luminescence spectroscopy of chrysoberyl, var. alexandrite

----

Two types of Cr^{3+} luminescence centers were found in alexandrite, R–lines at approximately 679 with 677.3 nm, and 694.4 with 691.7 nm, accompanied by N–lines of Cr–Cr pairs. These luminescence centers in the studied samples (Fig. 3B) are located at 644, 650, 653, 667, 669, 678, 680, 690, 694, 702, 707, and 716 nm. The luminescence band located at 702 nm may be attributed to V^{2+} (Gaft et al., 2005) although the V content was below the XRF detection limit but could be sufficient to induce luminescence.

The R–lines in chrysoberyl are divided to R_m (mirror, B2 octahedron) a R_i (inversion, B1 octahedron) which are located at 678 nm (R_m–line) a 690 nm (R_i–line). The luminescence band in the studied sample is shifted due to a chemical composition different to published. The region from 678 to 680 nm belong to R_m–line ($Cr^{3+}{}_{II}$) and 690 nm belong to R_i–line ($Cr^{3+}{}_I$) (Powell et al, 1985; Ollier et al., 2015). The N–lines are associated with Cr^{3+}– Cr^{3+} pairs (Solomonov et al., 2002): N_1 located at 702 nm is the most intensive, N_2 and N_3 at 707, 716 nm are weak. Luminescence intensity is increased with higher content Cr^{3+}. The most intensive luminescence duplet at 680 nm is caused by high Cr^{3+} content at the B2 site with C_s symmetry (Bordage et al., 2012).

The ratio between the R_m– a R_i–line intensities results from their different fluorescence decay time (Ollier et al., 2015). The decay times of R_m–line and R_i–line at 300 K are 290 and 48 μs, respectively (Powell et al, 1985). The intensity of the Cr^{3+} emission in the R_m–line depends on the iron content. As iron content increases, the emission signal of Cr^{3+} located at the mirror site decreases. Although it is difficult to evaluate quantitatively the amount of iron substituted at the mirror site, the Fe^{3+} proximity to Cr^{3+} leads to energy transfer between Cr^{3+} and Fe^{3+}. It results

in a shorter Cr^{3+} lifetime and lower R_m–line intensity. The luminescence spectrum of the studied chrysoberyl (ALM–1) with a high FeO content (2.63 wt. %) contains both R–lines in contrast to the sample Quilombo 2 with 2.41 wt.% FeO only (Ollier et al., 2015). We assume that the studied chrysoberyl (ALM–1) sample showed both lines due to significantly higher Cr_2O_3 content (0.72 wt.%) compared to Quilombo 2 with 650 ppm Cr (Ollier et al., 2015), despite higher iron content.

4.3 Spectra comparison

Chrysoberyl and spinel have slightly different structures with different topology although there are few similarities. In the spinel structure, Al^{3+} ions occupy tetrahedral and octahedral interstitial sites (Cynn et al., 1992). In chrysoberyl, Al^{3+} atoms are situated in slightly distorted octahedral voids of two types: B1 octahedra of Ci symmetry and B2 octahedra of Cs symmetry with different volumes – B2 > B1 (Urusov et al., 2011). The main difference is caused mainly by Be^{2+} and Mg^{2+} cations; Be^{2+} as smaller cation reduces chrysoberyl symmetry compared to spinel. Both cations belong to the second group in the periodic table, but there is a difference in properties because Be forms predominantly covalent compounds. Beryllium is most often in tetrahedral coordination; Mg prefers octahedral coordination (Housecroft & Sharpe, 2005).

The spinel structure is assigned to the cubic $Fd3m$ space group, the possible deviations are extremely small. The cations occupy the tetrahedral 8a sites with the T_d ($43m$) symmetry and the octahedral 16d site with the D_{3d} ($3m$) symmetry (Mikenda & Preisinger, 1981[a]; Mikenda & Preisinger, 1981[b]). All Al–O distances in a normal spinel (Mg) are near 1.93 Å (Brik et al., 2016), but there could be a certain degree of inversion.

Chrysoberyl crystallizes in the orthorhombic $Pbnm$ space group (Hazen, 1987). The Al^{3+} ions are octahedrally coordinated, occur in two inequivalent sites. In chrysoberyl, the unit cell contains four molecules with eight Al^{3+} ions (ionic radius of 0.535 Å) in distorted octahedral sites, and four Be^{2+} ions (ionic radius of 0.47 Å) in distorted tetrahedral sites (Scalvi et al., 2002). The Al^{3+} sites lying in the mirror plane (B2) have the site symmetry of the C_s point group (asymmetric molecules),
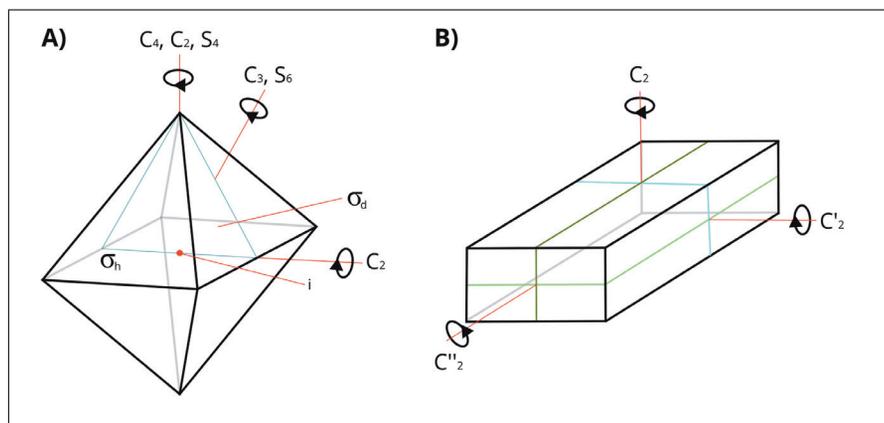
Fig. 4. Typical elements of symmetry (A) regular octahedron: point group O_h (*mm*) for the spinel (Vincent, 1977; www.chemtube3d.com); (B) regular rhombohedron: point group D_{2h} (mmm) for chrysoberyl – var. alexandrite (Mikenda & Preisinger, 1981[a,b], www.tulane.edu).

while Al^{3+} ions with inversion symmetry (B1) have C_i – molecules with identity and mirror plane cannot be distinguished whether they are horizontal or vertical symmetry planes (Fig. 4B) (Powell et al, 1985). Due to the small ionic radius of Be^{2+}, the chrysoberyl has crystal structure of lower symmetry then spinel. This property is also affecting a bond length in the Be–O 1.637 Å (Weber et al., 2007). The six oxygen ligands produce a crystal structure which can be described as having O_h point group, slightly distorted to C_s symmetry (Powell et al, 1985). The Al–O bond length at the B2 (1.938 Å) sites is larger than at the B1 (1.890 Å) sites, because B2 is wider at that site than at B1 (Weber et al., 2007).

Spinel has higher symmetry than chrysoberyl. Symmetry operations in spinel include: (A) several C_n n–fold rotational axes and rotationally–reflecting operations /stepless rotations (rotation about the axis of rotation at an angle of 2π / n and in the plane of reflection perpendicular to this axis) S_n; (B) planes of symmetry σ_d (the vertical plane of symmetry sweeps the angle between two double axes perpendicular to the principal axis) dihedral plane of symmetry, and σ_h (planes of symmetry is perpendicular to the principal axis) horizontal plane of symmetry (Fig. 4A). Chrysoberyl has fewer symmetric elements than spinel because the *mmm* space group contains only three rotational axes C_n and three perpendicular planes (Vincent, 1977).

From the symmetry of studied oxides, the influence of the structure on luminescence spectra can be evidenced. Luminescence bands in spinel spectrum are narrower and better defined than in chrysoberyl, in which these partly overlaps. This is caused by the splitting of allowed electronic states due to lower symmetry of the structure and the crystallographic sites containing Cr^{3+} in chrysoberyl (Powell et al, 1985). Another difference in spectra of both minerals is observed in the intensity of the most intensive R lines at 680–690 nm.

5. CONCLUSIONS

- -

The comparison of Cr^{3+} luminescence spectra of two oxide minerals with relatively similar but sufficiently different crystal structures showed the influence of the structural complexity and symmetry on the luminescence. In general, lower symmetry of the structure and the Cr^{3+}–bearing octahedra results in splitting, widening and overlapping of the luminescence bands in spectrum. Spinel with higher symmetry than chrysoberyl, var. alexandrite has the luminescence spectrum with smaller number of better resolved bands.

References

Anthony J.W., Bideaux R.A., Bladh K.W. & Nichols M.C., 2017: Handbook of Mineralogy. Mineralogical Society of America. Chantilly, VA 20151–1110, USA. http://www.handbookofmineralogy.org/.

Bordage A., Rossano S., Horn A.H. & Fuchs Y., 2012: Site partitioning of Cr^{3+} in the trichroic alexandrite $BeAl_2O_4$:Cr^{3+} crystal: contribution from X–Ray absorption spectroscopy. *Journal of Physics,* 24, 225401–225409.

Bosi F., Biagioni C. & Pasero M., 2019: Nomenclature and classification of the spinel supergroup. *European Journal of Mineralogy, 31*, 183–192.

Brik M.G., Papan J., Jovanović D.J. & Dramićanin M.D., 2016: Luminescence of Cr^{3+} ions in $ZnAl_2O_4$ and $MgAl_2O_4$ spinels: correlation between experimental spectroscopic studies and crystal field calculations. *Journal of Luminescence,* 177, 145–151.

Burshtein Z., Henderson D.O., Morgan S. & Silberman E., 1989: Vibrational spectra of chrysoberyl ($BeAl_2O_4$). *Journal of Physics and Chemistry of Solids,* 50, 1095–1100.

Cynn H., Sharma S.K., Cooney T.F. & Nicol M., 1992: High–temperature Raman investigation of order–disorder behavior in the $MgAl_2O_4$ spinel. *Physical Review B,* 45, 500–502.

Derkosch J., Mikenda W. & Preisinger A., 1977: N–Lines and Chromium–Pairs in the Luminescence Spectra of the Spinels $ZnAl_2O_4$: Cr^{3+} and $MgAl_2O_4$: Cr^{3+}. *Journal of Solid State Chemistry,* 22, 127–133.

Gaft M., Reisfeld R. & Panczer G., 2015: Modern Luminescence Spectroscopy of Minerals and Materials. Springer, 606 p.

Hazen R.M., 1987: High–pressure crystal chemistry of chrysoberyl, Al_2BeO_4: insights on the origin of olivine elastic anisotropy. *Physics and Chemistry of Minerals,* 14, 13–20.

Hawthorne F.C. & Huminicki D.M.C., 2002: The Crystal Chemistry of Beryllium. *Reviews in Mineralogy and Geochemistry,* 50, 333–403.

Housecroft C.E. & Sharpe A.G., 2005: Inorganic Chemistry. Second Edition. Pearson Prentice Hall, ISBN 0130–39913–2, 949 p.

Chopelas A. & Hofmeister A.M., 1991: Vibrational spectroscopy of aluminate spinels at 1 atm and of $MgAl_2O_4$ to over 200 kbar. *Physics and Chemistry of Minerals,* 18, 279–293.

[a]Mikenda W. & Preisinger A., 1981: N–Lines in the luminescence spectra of Cr^{3+}–doped spinels (i) identification of n–lines. *Journal of Luminescence*, 26, 53–66.

[b]Mikenda W. & Preisinger A., 1981: N–Lines in the luminescence spectra of Cr^{3+}–doped spinels (ii) origins of n–lines. *Journal of Luminescence*, 26, 67–83.

Mohler R.L. & White W.B., 1995: Influence of Structural Order on the Luminescence of Oxide Spinels: Cr^{3+}–Activated Spinels. *Journal of The Electrochemical Society,* 11, 3923–3927.

Ollier N., Fuchs Y., Cavani O., Horn A. & Rossano S., 2015: Influence of impurities on Cr^{3+} luminescence properties in Brazilian emeralds and alexandrite minerals. *European Journal of Mineralogy,* 27, 783–792.

Phan T.L., Phan M.H. & Yo S.Ch., 2004: A New Band in Cr^{3+}–doped $MgAl_2O_4$ natural spinel at room temperature. *Physica Status Solidi B,* 241, 434–438.

Powell R.C., Xi L., Gang X., Quarles G.J. & Walling J.C., 1985: Spectroscopic properties of alexandrite crystals. *Physical Review B*, 32, 2788–2797.

Scalvi R.M.F., Ruggiero L.O. & Li M.S., 2002: Influence of annealing on X–ray diffraction of natural alexandrite. *Powder Diffraction,* 17, 136–138.

Shannon R.D., 1976: Revised Effective Ionic Radii and Systematic Studies of Interatomic Distances in Halides and Chalcogenides. *Acta Crystallographica A*, 32, 751–767.

Slotznick S.P. & Shim S.H., 2008: In situ Raman spectroscopy measurements of $MgAl_2O_4$ spinel up to 1400°C. *American Mineralogist*, 93, 470–476.

Solomonov V.I., Mikhailov S.G. & Lipchak A.I., 2002: Impurity luminescence of alexandrite crystals. *Journal of Applied Spectroscopy,* 69, 423–429.

Urusov V.S., Gromalova N.A., Vyatkin S.V., Rusakovn V.S., Maltsev V.V. & Eremin N.N., 2011: Study of structural and valence state of Cr and Fe in chrysoberyl and alexandrite with EPR and Mössbauer spectroscopy. *Moscow university Geology Bulletin,* 66, 102–107.

Vincent A., 1977: Molecular symmetry and group theory. John Wiley & Sons, London, 191 p.

Weber S.U., Grodzicki M., Lottermoser W., Redhammer G.J., Topa D., Tippelt G. & Amthauer G., 2007: [57]Fe Mössbauer Spectroscopy, X–Ray Single Crystal Diffractometry and Electronic Structure Calculations on Natural Alexandrite. *Physics and Chemistry of Minerals*, 34, 507–515.

Weiyi J., Qingrong Z., Yusheng S., Yanyun W., Zhenyi Y. & Shouan H., 1985: Raman spectra of chrysoberyl Al_2BeO_4. *Chinese Science Bulletin*, 30, 452.

White W.B., Roy R. & Crichton J.M., 1967: The "Alexandrite effect": and optical study. *The American Mineralogist,* 52, 867–871.

Yeom T.H., Choh S.H., Honhg K.S., Yeom H.Y., Park Y.H. & Yu Y.M., 1998: Nuclear Quadrupole Interactions of [27]Al in Alexandrite Single Crystal. *Zeitschrift für Naturforschung PT B,* 53, 568–572.

Yeom T.H. & Choh S.H., 2001: Cr^{3+} (I) and Cr^{3+} (II) Centers in Alexandrite Single Crystal. *Journal of Applied Physics*, 90, 5946–5950.

https://www.chemtube3d.com/octahedral–sulfur–hexafluoride–sf6–symmetry/ [19.9. 2019 10:59].

https://www.tulane.edu/~sanelson/eens211/32crystalclass.htm [20.9. 2019 8:58].